PHYSICAL REVIEW C VOLUME 20, NUMBER 2 AUGUST 1979

Pre-equilibrium neutron emission for the ^{164}Dy$(\alpha,xn\,\gamma)^{168-x}$Er reaction studied by n-γ coincidence measurements

H. Sakai
Research Center for Nuclear Physics, Osaka University, Suita, Osaka 565, Japan

H. Ejiri,* T. Shibata, Y. Nagai, and K. Okada
Department of Physics, Osaka University, Toyonaka, Osaka 560, Japan

(Received 30 March 1979)

Neutron deexcitation mechanism through pre-equilibrium and equilibrium phases of the ^{164}Dy$(\alpha,xn\,\gamma)$ reaction at $E(\alpha) = 120$ MeV was studied as a function of the neutron multiplicity x. The deexciting neutrons with a wide range of the multiplicity x showed energy and angular distributions characteristic of the pre-equilibrium process followed by equilibrium evaporation. The pre-equilibrium neutrons were found to carry away considerable amounts of angular momenta. The energy and angular distributions of the emitted neutrons were analyzed in terms of a simple two phase deexcitation model of the pre-equilibrium phase and the equilibrium phase. It gives the mean number of pre-equilibrium neutrons ($\sim$1.7), pre-equilibrium quasitemperature ($\sim$6 MeV), the average exciton particles number around 20, and the equilibrium temperature (1.6 MeV).

[NUCLEAR REACTIONS ^{164}Dy$(\alpha,xn\,\gamma)^{168-x}$Er, x=6–11, $E(\alpha)$=120 MeV; measured $\sigma(x)$, $\sigma(E_n,\theta_n)$; deduced angular momentum removal by neutrons, pre-equilibrium effects, properties of pre-equilibrium phase. Two phase deexcitation model analysis. Enriched target.]

I. INTRODUCTION

Nuclear reactions induced by medium energy projectiles (~30 MeV/nucleon) are interesting in view of pre-equilibrium and equilibrium deexcitation processes. The highly excited (~100 MeV) nuclear system produced by the projectile bombardment decays first by emitting a number of fast nucleons at the pre-equilibrium stage and later by evaporating low-energy nucleons at the equilibrium stage. Recently high-energy tails of charged particle spectra and excitation functions well above the reaction threshold have been investigated to study the pre-equilibrium deexcitation process.[1]

Major reaction channels for medium-energy (~100 MeV) light particles interacting with heavy nuclei are (particle, $xn\gamma$) reactions with a large variety of neutron multiplicities ($x = 2-12$). Here one may expect some fast neutrons at the pre-equilibrium stage followed by much low-energy neutron evaporation. There have, however, not been many neutron measurements. Some studies of singles spectra of neutrons following equilibrium[2-5] and pre-equilibrium[6-8] reactions have been reported. A simple schematic diagram of the $(\alpha,xn\gamma)$ deexcitation process is shown in Fig. 1. The quantity E_T is an energy sum of the emitted neutrons. The pre-equilibrium process may be manifest in reactions with a small number of multiplicity x where a small number of fast neutrons are emitted, while the equilibrium process is relatively important in reactions with a large multiplicity x of the evaporating neutrons.

It is important to investigate fast and slow neutrons following (particle, $xn\gamma$) reactions as a function of the neutron multiplicity x in order to study deexcitation processes through the pre-equilibrium to equilibrium phases of the reaction. Here the neutron multiplicity x can be identified by requiring a coincidence with discrete γ rays (γ_x) characteristic of the (particle, $xn\gamma_x$) reaction residues. This type of n-γ coincidence study was first carried out by Ejiri et al.[9] They studied in detail ^{165}Ho$(p,xn\gamma)$Er reaction at $E_p = 60$ MeV, and found properties of the neutrons emitted at the pre-equilibrium stage. Since the projectile used was 60 MeV protons, the neutron multiplicity x was limited to $x = 4-6$, and the angular momentum involved was rather small.

The (particle, $xn\gamma$) reaction mechanism has also been studied by singles γ ray and coincidence γ-γ measurements. Recently γ-ray multiplicities for $(\alpha,xn\gamma)$ reactions and the median spin value of the ground state rotational band have been found to saturate as the projectile energy increases well beyond the threshold energy.[10-13] This suggests that a considerable fraction of the input angular momentum is carried away by the pre-equilibrium neutrons.

The purpose of the present work is to extend the previous $(p,xn\,\gamma)$ reaction induced by 60 MeV protons to the $(\alpha,xn\,\gamma)$ reaction induced by 120 MeV α particles. Here the range of the neutron mul-

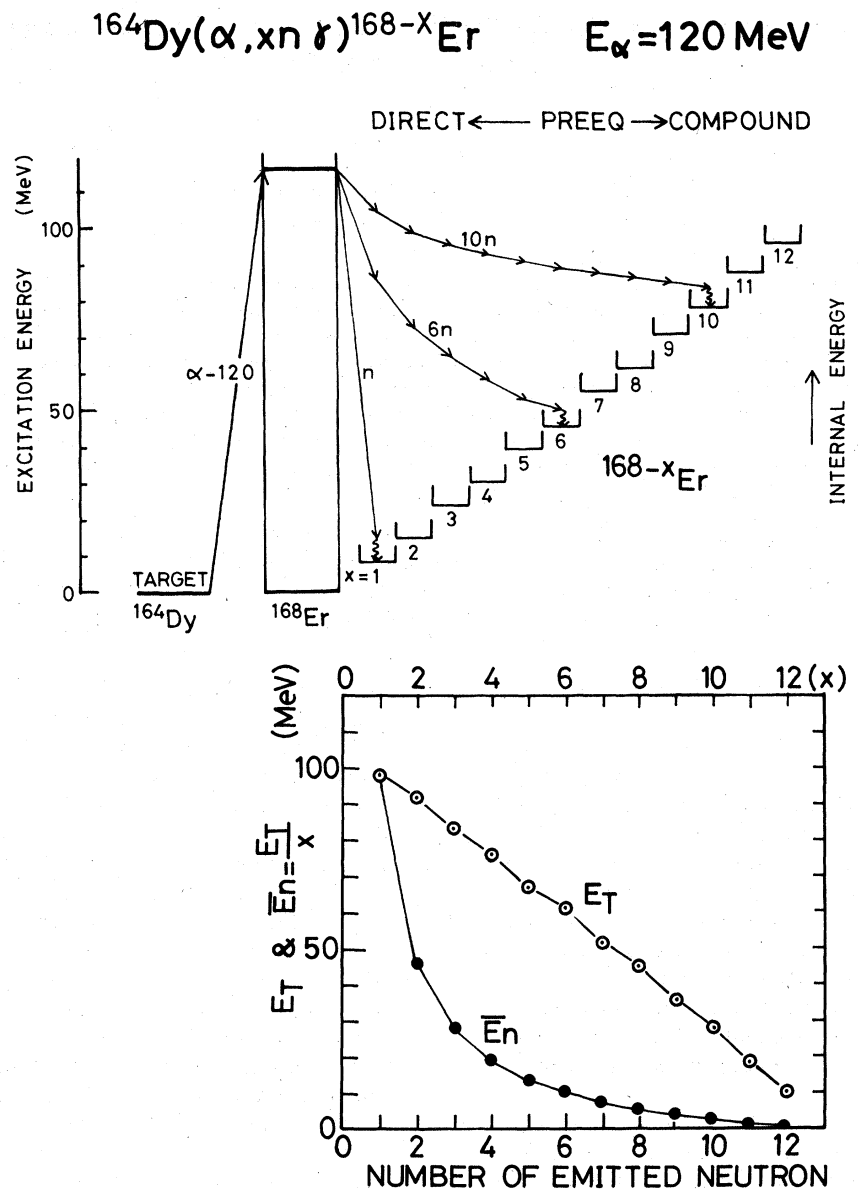

FIG. 1. Schematic energy levels and deexcitation processes for the $^{164}Dy(\alpha, xn\,\gamma)$ reactions at $E(\alpha) = 120$ MeV (upper part) and the total energy E_T of the emitted neutrons and the average kinetic energy $\bar{E}_n = E_T/x$ per neutron (see text) as a function of the emitted neutron multiplicity x.

tiplicity is much larger and the angular momentum involved is also much larger. We studied characteristic behavior of neutrons emitted through the pre-equilibrium and equilibrium stages as a function of the neutron multiplicity x in a wide range ($x = 4$–11). Energy, angular, and multiplicity distributions of the neutrons give effective energy parameter (quasitemperature), the active exciton particles (local mass), and the multiplicity for the deexciting neutrons at the pre-equilibrium stage. These data may yield the role of pre-equilibrium neutrons in the angular momentum removal. Thus one gets the missing link in the angular momentum balance as suggested from the γ-γ coincidence works.[10-13]

The $^{164}Dy(\alpha, xn\gamma)^{168-x}Er$ reactions with $x = 4$–11 were used, since the residual Er isotopes were well known rotors, and the neutron multiplicities (reaction channels) were well defined by coincidence with the rotational γ_x rays characteristic of $^{168-x}Er$.

Similar (particle, $xn\gamma$) reactions induced by heavy ions are interesting in comparison with the light-ion induced reactions. The neutron-coin-

cidence experiments for the ^{169}Tm(^{14}N, $xn\gamma$) reactions at $E(^{14}\text{N}) = 130$ MeV (~9 MeV/nucleon) showed that the neutrons came mostly from the equilibrium stage,[14] and γ-ray spectra following the ^{169}Tm(^{14}N, $xnyp\gamma$) reaction at $E(^{14}\text{N} = 210$ MeV (15 MeV/nucleon) showed an important role in particle emission at the pre-equilibrium stage.[15] Quite recently Westerberg *et al.* have carried out an extensive n-γ coincidence measurement for the ^{158}Gd(^{12}C, $xn\gamma$) reaction at $E(^{12}\text{C}) = 152$ MeV (Ref. 16) (13 MeV/nucleon). They found some pre-equilibrium neutrons there.

We describe our experimental procedures in Sec. II, and the results in Sec. III. The observed features are analyzed in terms of the pre-equilibrium process, followed by the equilibrium evaporation in Sec. IV. In the last section we summarize our results.

II. EXPERIMENTAL PROCEDURES

Incident α particles of 120 MeV energy were provided by the 230 cm AVF cyclotron at the RCNP (Research Center for Nuclear Physics) Osaka University. The ^{164}Dy target with 3.3 mg/cm^2 in thickness was prepared by depositing enriched ^{164}Dy oxide powder onto a 0.003 mm Mylar film. The isotopic enrichment of the target was 98.4%.

First we measured an accurate singles γ-ray spectrum at 125° in order to get cross sections $\sigma(x)$ of the various $(\alpha, xn\gamma)$ reactions with a wide range of the neutron multiplicity x. The detector used was a pure Ge detector with $\Delta E = 1$ keV for 511 keV γ rays. The $(\alpha, xn\gamma)$ reaction cross sections leading to even Er isotopes were obtained from the yields of the ground band $2^+ \rightarrow 0^+$ γrays, and those for odd Er from the γ-ray yields along the yrast, yrare, and other possible bands by referring to γ-ray branching ratios observed in previous in-beam works.[17-24] The internal conversion electrons were corrected for. The counting rate was always kept below 700 counts/s, so that no dead time correction was necessary.

Angular and energy distributions for the decay neutrons were measured at 35°, 62.5°, 90°, and 145° in coincidence with rotational rays characteristic of the reaction residues. A 12.7×12.7 cm NE213 liquid scintillator was set at 24 cm from the target to detect neutrons which were separated from γ rays by a pulse shape analysis method.[25] A 2 cm lead absorber was used in front of the NE213 to reduce γ rays. The lead absorber affected slightly the neutron spectrum. The effect of the absorber was corrected for by measuring the neutron TOF (time of flight) spectra with and without the lead absorber. The light output of the scintillator was calibrated by measuring the Compton edge of γ rays following ^{56}Co, ^{88}Y, and ^{22}Na isotopes and by using the Verbindki table.[26] The accuracy of neutron energy was obtained to 10% by converting the light output for electrons to that for neutrons (namely for recoiling protons). The neutron energy spectrum was obtained by unfolding the measured neutron (recoil proton) pulse height spectrum as in Ref. 27. The energy resolution was around 1–2 MeV for 4-15 MeV neutrons. Owing to the large solid angle of the NE213 neutron detector, the pileup effect in the detector was estimated to be at most a few percent.

Background contribution due to lead shields and other surroundings to the neutron detector was examined and found to be negligible in the present coincidence experiment. The γ rays for the n-γ coincidence measurement were detected at 90° by a 55 cm^3 Ge(Li) detector at a distance of 16 cm from the target. The singles counting rate of the liquid scintillator and the Ge(Li) detector at a typical run were 6.0×10^3 and 2.2×10^3 counts/s, respectively. The accidental coincidence rate was less than 1%. Correction for the n-γ angular correlation were not applied. The energy and timing signals of the neutrons and γ rays were recorded in an event-by-event mode on a magnetic tape via an on-line data acquisition system (Raw Data Processor + PDP11/40).[28]

The present method having a large solid angle (0.3 sr) is suitable for the n-γ coincidence measurement to obtain rough shapes of the neutron energy spectra characteristic of the pre-equilibrium and equilibrium processes. The extracted neutron energy spectrum was checked to be consistent with that obtained by a time of flight method.[29]

III. RESULTS AND ANALYSIS

A. Cross sections for the ^{164}Dy $(\alpha, xn\,\gamma)$ reactions

The observed absolute cross sections are shown as a function of the neutron multiplicity x and/or the ground state Q values in Fig. 2. The dotted and dashed lines in Fig. 2 were evaluated for an equilibrium process alone in a framework of a simple statistical model. The nuclear temperature used is $T = (U/a)^{1/2}$, where U is the excitation energy of the residual nucleus and a is given by $A/10$ MeV^{-1}.[30,31] As the excitation energy decreases through the neutron evaporation, the temperature decreases. Thus the average temperature T_e all through the neutron evaporation is roughly given by $T_e = \frac{2}{3}T_0$, where T_0 is the initial temperature after the first neutron evaporation. It is estimated from the excitation energy $U = E_\alpha^{\text{c.m.}} + Q(\alpha, n) - 2T_0$, where $E_\alpha^{\text{c.m.}}$ is the projectile energy

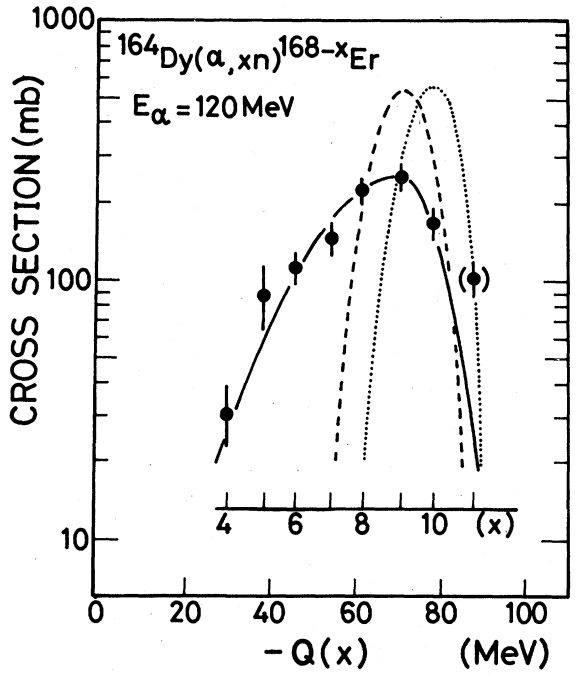

FIG. 2. Absolute cross sections for the ^{164}Dy$(\alpha, xn\,\gamma)$ $^{168-x}$Er reactions as a function of the neutron multiplicity x and/or the ground state Q values. The solid line is the present calculation (see text). The dotted and dashed lines are evaluated for the equilibrium process alone with the nuclear temperatures $T_e = 1.7$ and 2.2 MeV, respectively.

in the center-of-mass system, $Q(\alpha, n)$ is the (α, n) reaction Q value, and $2T_0$ is the mean kinetic energy of the neutron. We obtained $T_0 = 2.5$ MeV and $T_e = 1.7$ MeV for initial and average equilibrium temperature, respectively. The cross sections for various $(\alpha, xn\,\gamma)$ reaction channels (neutron multiplicity x) for the equilibrium evaporation model were calculated as shown in Ref. 9 by using for simplicity the average temperature T_e. For comparison we show also a curve calculated by using the $T_e = 2.2$ MeV corresponding to the extreme case of the Fermi gas.

The observed $\sigma(x)$ (the neutron multiplicity distribution) is shifted much towards smaller x from the expectation for the equilibrium evaporation process. This indicates an important role of the fast neutron emission at the pre-equilibrium stage in the region of the small x ($x \leq 8$).

B. Neutrons following the ^{164}Dy $(\alpha, xn\,\gamma)$ $^{168-x}$Er reaction

Typical γ-ray spectra observed in coincidence with neutrons detected at 35° (lab) are shown in Fig. 3. The labels A–H in the figure stand for the γ-ray spectra gated by the eight recoil proton energy windows in the liquid scintillator. The energy intervals for A, B, and H are 2.5–3.5, 3.5–5.1, 5.1–6.8, 6.8–9.8, 9.8–12.4, 12.4–15.0, 15.0–17.6, and 17.6–20.1, all in MeV units, respectively. The neutron pulse-height spectra for various neutron multiplicities x were obtained from yields of the neutron pulses in coincidence with the yrast band γ_x rays following the $(\alpha, xn\,\gamma)$ reactions. The neutron energy spectrum was extracted by unfolding the observed neutron pulse-height spectrum.[27] Here use was made of the calculated response functions which were found to be adequate by measuring them for monoenergetic neutrons selected by a time of flight method.[27] The absolute neutron cross sections for the (α, xn) reactions leaving even-even Er isotopes are easily obtained from the neutron spectra gated by the ground band $4^+ \rightarrow 2^+$ γ rays, since the $4^+ \rightarrow 2^+$ γ-ray yields stand almost for the total reaction yields (see the singles γ-ray spectra). The extracted neutron energy spectra for the $(\alpha, 10n)$, $(\alpha, 8n)$, and $(\alpha, 6n)$ reactions are plotted in Fig. 4. The arrows in Fig. 4 indicate the mean neutron energy

$$\bar{E}_n = \frac{E_T}{x} = \frac{E_\alpha^{\text{c.m.}} + Q^{\text{eff}}(x)}{x}, \tag{1}$$

where Q^{eff} is the effective Q value for the $(\alpha, xn\,\gamma)$ reaction. Q^{eff} is given as $Q^{\text{eff}} = Q^0 - E_\gamma$, where Q^0 is the ground state Q value and E_γ is the mean excitation energy of the residual nucleus. We use the value $E_\gamma = 10.7$ MeV by correcting for the rotational energy of the yrast level in the present spin region.

The obtained neutron energy spectra (Fig. 4) consists of a high-energy tail around 10–15 MeV characteristic of the pre-equilibrium process and a low energy evaporation pattern. The former is enhanced at forward angles in the (α, xn) reactions with small x as shown in Fig. 4. Forward peaking angular distributions for the individual reaction channels are well illustrated in Fig. 5. The forward peaking angular distributions are mainly due to the high-energy tails as shown in Fig. 5. The observed neutron spectra for the (α, xn) reactions of small neutron multiplicities x differ obviously from just singles neutron spectrum for all neutrons following much slower (heavy-ion) projectiles.[2-5] Note that the mean neutron energies $\bar{E}_n$ (Fig. 4) given from the reaction Q values [Eq. (1)] for the $(\alpha, 8n)$ and $(\alpha, 6n)$ reactions are as large as 6 and 10 MeV, respectively. The low-energy parts are consistent with the $\sigma(E) \propto E_n \exp(-E_n/T_e)$ with $T_e = 1.5 \sim 2$ MeV as expected for the neutron evaporation from the 50–80 MeV excitation region. The high-energy tail for the pre-equilibrium $(\alpha, 6n)$ reaction extends beyond the present upper limit (20 MeV) at forward angles. These neutron spectra suggest that the present reaction

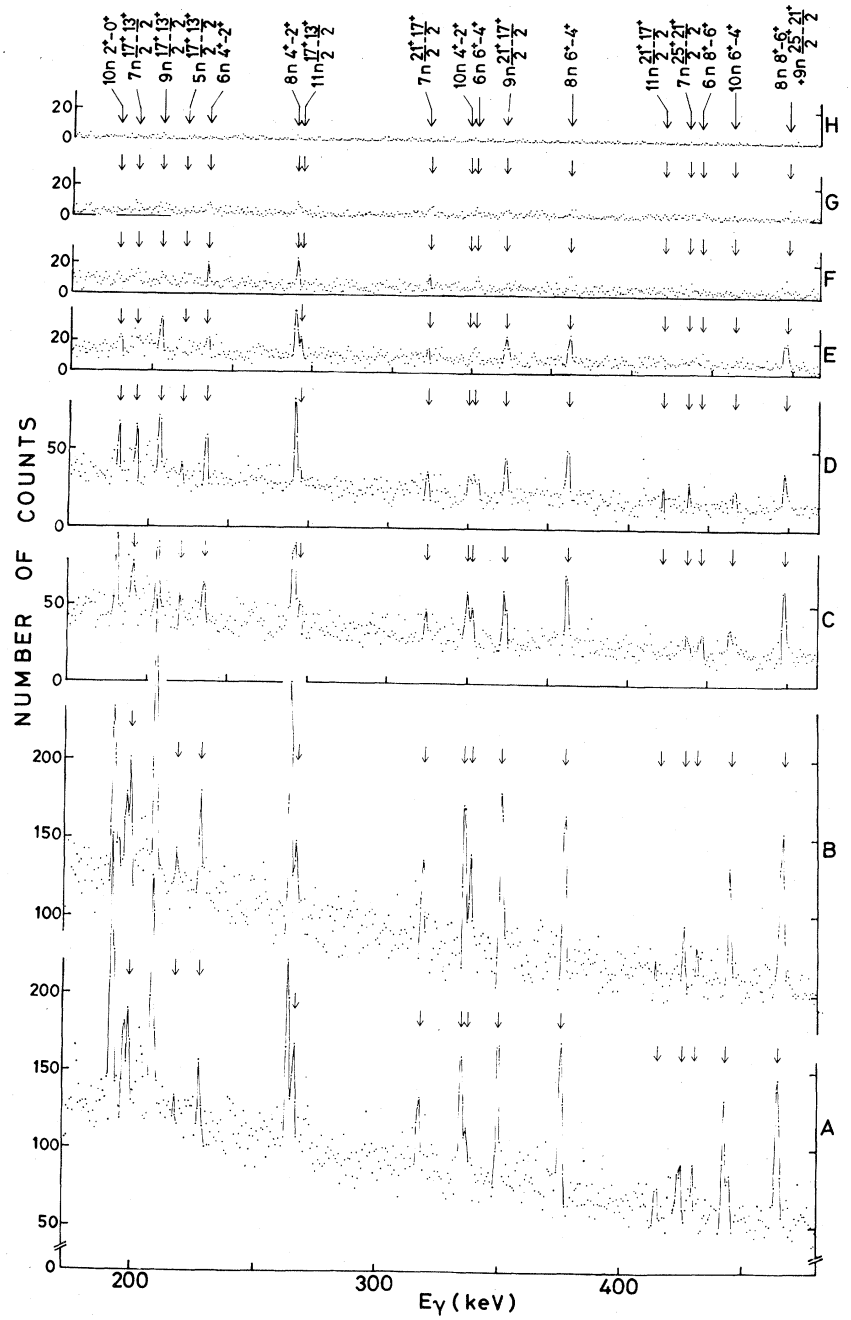

FIG. 3. γ-ray spectra in coincidence with the neutrons. The labels A–H stand for the eight recoil proton energy (pulse height) windows in the liquid scintillator (see text).

may be described in terms of a two phase deexcitation process: One is the pre-equilibrium process which is respondible for the high-energy component, and the other is the equilibrium process (evaporation) which is responsible for the low-energy component in neutron spectra.

Finite contributions of the pre-equilibrium neutrons to most of the (α, xn) reactions are clearly illustrated by a large asymmetry of the neutron angular distribution with respect to 90°. The asymmetry coefficients A_1, for the $A_1P_1(\cos\theta)$ term in the Legendre expansion $\Sigma A_i P_i(\cos\theta)$ are 0.74 ± 0.26, 0.64 ± 0.15, 0.55 ± 0.05, 0.63 ± 0.15, 0.56 ± 0.10, and 0.3 ± 0.2 for $x = 6$, 7, 8, 9, 10, and 11,

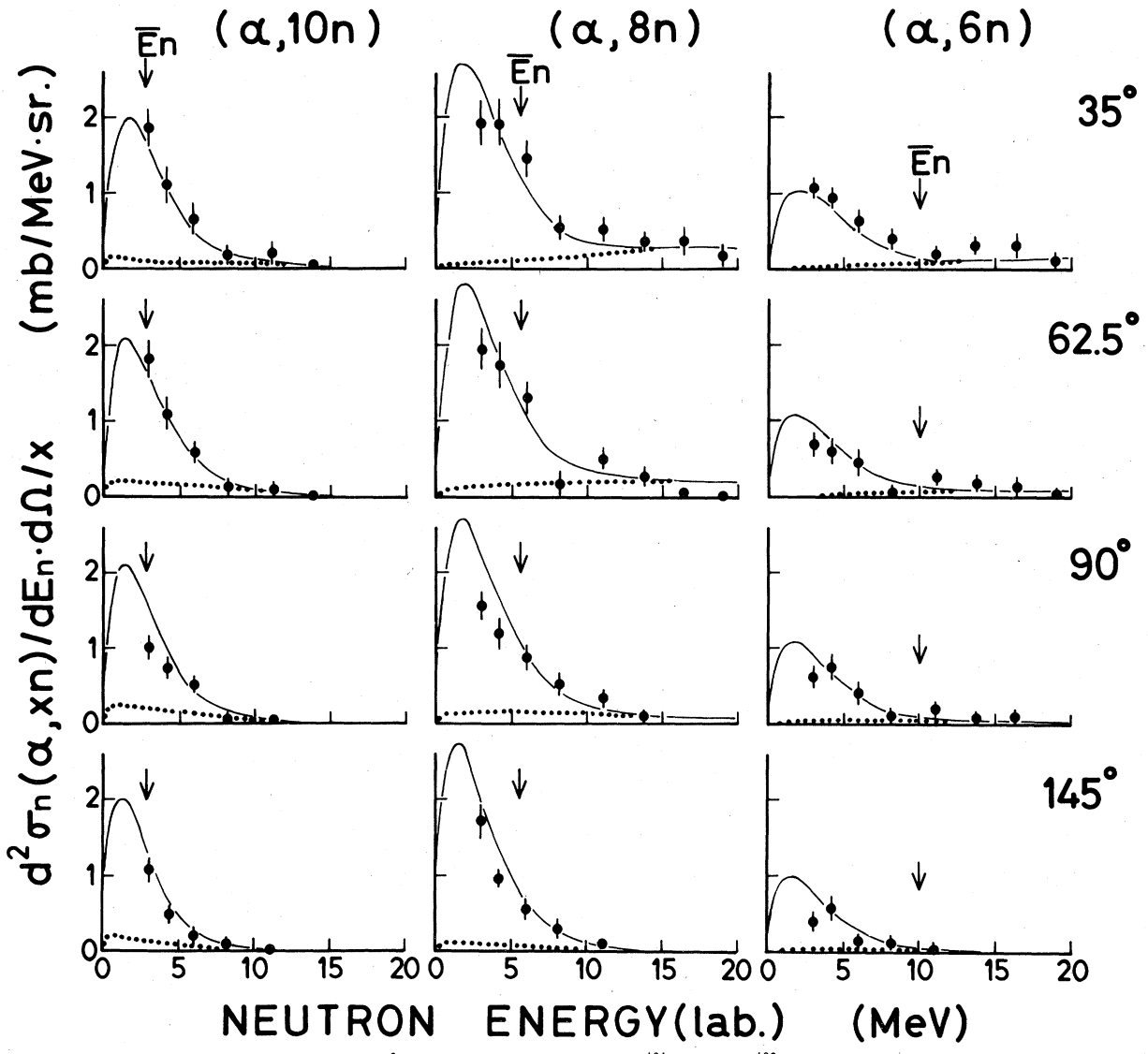

FIG. 4. Neutron energy spectra $[d\sigma_n{}^2(\alpha,xn)/d\Omega\, dE_n]/x$ for the ^{164}Dy$(\alpha,xn)^{168-x}$Er reactions as a function of the neutron multiplicity x detected at $\theta_{lab}=35°$, 62.5°, 90°, and 145°. Solid lines are the present calculations. The dotted lines are contributions from the pre-equilibrium process. The arrows indicate the mean neutron energy $\overline{E}_n$. Only statistical errors are indicated.

respectively. They are plotted in Fig. 6. A dashed line in Fig. 6 was evaluated by using a relation $A_1=2(V'/V_b)$ as was given in Ref. 9. The V' is the velocity of the center-of-total mass and V_b is the velocity of the emitted neutron in the center-of-mass frame. The V_b was obtained from the mean neutron energy $\overline{E}_n$ given by Eq. (1).

It is interesting to note that the values A_1x are almost constant in a wide range of the neutron multiplicity as shown in Fig. 7.

Correcting for the contribution of the finite velocity of the center of mass to the $A_1P_1(\cos\theta)$ term in the present neutron energy, we get an asymmetry coefficient $A_1x\approx 4.0$. A pure equilibrium (compound) process would give always a symmetric angular distribution with respect to 90°. Therefore the finite values of the $A_1P_1(\cos\theta)$ do indicate quantitatively neutron asymmetry in the center-of-mass system due to the pre-equilibrium process. According to a simple pre-equilibrium deexcitation model used in the previous work,[9] one gets

$$A_1(\mathrm{pe})x\approx 4n_p[E_\alpha/E_n(\mathrm{pe})]^{1/2}/A',$$

where n_p, A', $E_n(\mathrm{pe})$, and E_α are the number of pre-equilibrium neutrons, the mean number of ex-

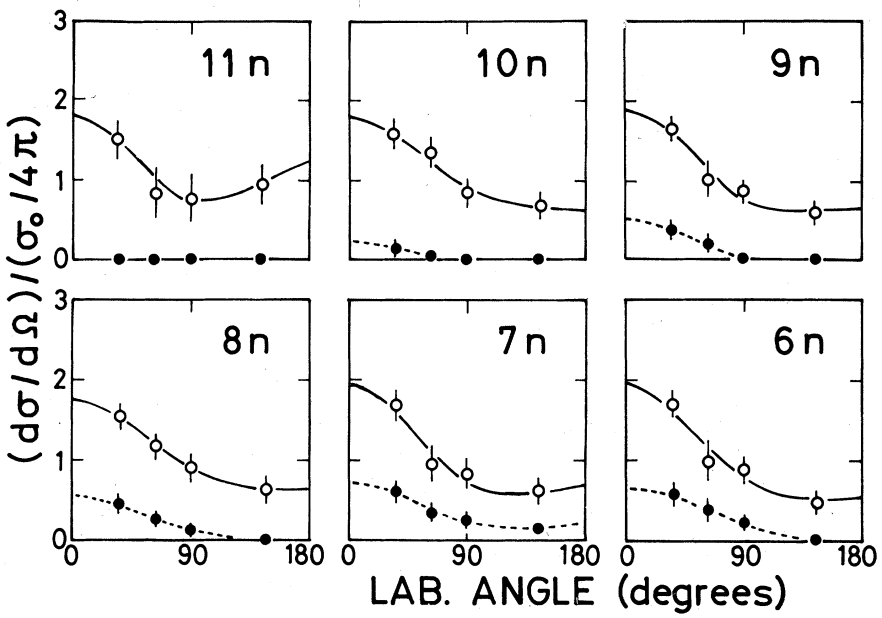

FIG. 5. Energy-integrated angular distributions of neutrons for the ^{164}Dy$(\alpha,xn)^{168-n}$Er reactions with $x=6-11$. Open and closed circles are the data points for all neutrons above 2.5 MeV and those for fast neutrons above 9.8 MeV, respectively. Solid and dashed lines are curves for least square fits.

citon particles at the pre-equilibrium stage, their mean energy in this local A' system (high-energy components in neutron spectra), and the incident energy, respectively. Assuming the observed E_n values (see Fig. 4) and inserting the observed $A_1(\text{pe})\cdot x$ values, we get the n_p/A' values given in Table I. The n_p/A' increases 1/4.0 for the $(\alpha,10n)$ reaction to 1/2.4 for the $(\alpha,6n)$ reaction and this is due to the increase of the pre-equilibrium neutron number n_p and the decrease of active exciton particle number A' at the pre-equilibrium phase as the neutron multiplicity decreases. These values are roughly in accord with the exciton model evaluations of $n_p \approx 2$ and $A' = 6$–10.[32,33]

It is interesting to note that in Figs. 4 or 5 low-energy parts of the neutron spectra do not show a strong angular dependence. It implies that the γ-ray spectra gated by high-energy neutrons at the forward angles may be dominated by the pre-equilibrium process, while the γ rays gated by the low-energy neutrons at the backward angles

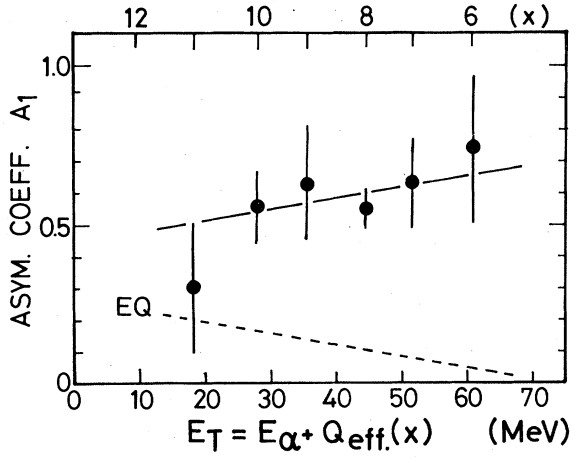

FIG. 6. The asymmetry coefficient A_1 for the $A_1P_1(\cos\theta)$ term in the Legendre expansion $\sum_i A_i P_i(\cos\theta)$ of neutrons following the ^{164}Dy(α,xn)Er reactions. They are plotted as a function of the total kinetic energy E_T and/or the neutron multiplicity x. The dashed line is calculated for the equilibrium process alone. The solid line is just to show a general trend.

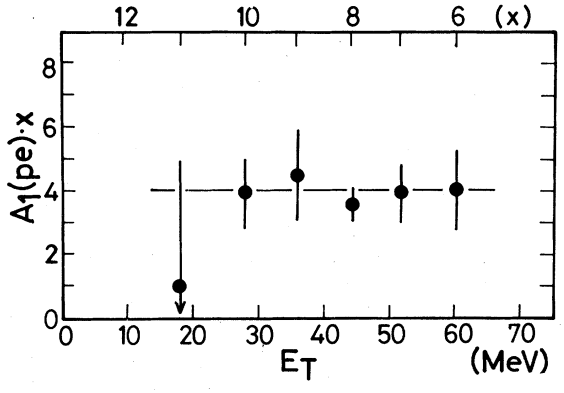

FIG. 7. The values for $A_1(\text{pe})\cdot x$ where $A_1(\text{pe})$ is the net asymmetric term and x is the neutron multiplicity, as a function of the neutron multiplicity x and/or the total kinetic energy E_T. The solid line is drawn to guide the eyes (see text).

TABLE I. Ratios of the number of pre-equilibrium neutrons to active exciton particles (local mass). A_1(exp), A_1(c.m.), and A_1(pe) are the asymmetry coefficients for the experimental result, the contribution due to center-of-total mass velocity, and the net pre-equilibrium process, respectively.

Reaction	A_1(exp)	A_1(c.m.)[a]	A_1(pe)	A_1(pe)$\cdot x$	E_n(pe) (MeV)[b]	n_p/A'
$(\alpha, 10n)$	0.54± 0.11	0.16	0.38	3.8	8	1/4.0
$(\alpha, 8n)$	0.55± 0.06	0.10	0.45	3.6	14	1/3.2
$(\alpha, 6n)$	0.74± 0.25	0.04	0.70	4.2	18	1/2.4

[a] From the evaluation according to Ref. 9 (see text).
[b] Assumed by using the high-energy components in Fig. 4.

may be dominated by a compound process with large neutron multiplicity. This feature can be demonstrated in Fig. 8. Here the γ-ray spectra gated by fast neutrons above 6.8 MeV at 35° and all neutrons above 2.5 MeV at 145° are shown. A drastic enhancement of the $(\alpha, 6n)$ γ-ray lines in comparison with those of the $(\alpha, 10n)$ reaction is obtained. Thus the γ rays for the small number of the neutron multiplicity are prominent in the spectrum gated by the high-energy neutrons at forward angles. On the other hand, if we detect γ rays in coincidence with backward neutrons, the γ-ray spectrum is dominated by reaction channels with a large neutron multiplicity. Thus the γ-ray spectrum gated by the backward neutrons may be useful to study properties of nuclei far from the region of β stability.

Inamura *et al.*[35] studied yrast γ rays following the ^{159}Tb(^{14}N, αxn)$^{169-x}$Yb reaction in coincidence with direct and compound α particles. They found that the high-energy α particles emitted at forward angles populate a narrow range of spin values in the residual nuclei, while low-energy α particles emitted at backward angles populate a wide range of spin values. The yrast band γ-ray intensities for the $(\alpha, 10n)$, $(\alpha, 8n)$, and $(\alpha, 6n)$ reactions are plotted against the yrast level spin values in Fig. 9. The γ-ray intensities were corrected for the detection efficiencies of the Ge(Li) detector and conversion electron. The intensities for the $(\alpha, 8n)$ reaction obtained from the singles γ-ray spectrum are also shown in Fig. 9 as solid lines in each reaction channel for comparison. No appreciable difference was found in all reaction channels between the γ-ray transition intensities gated by the forward high-energy neutrons, backward neutrons, and the intensities obtained from the singles spectrum, although the $(\alpha, 10n)$ reaction is considered to involve less contributions from the pre-equilibrium process than the $(\alpha, 6n)$ reaction. The yrast band transition intensities for the $(\alpha, 10n)$ reaction, however, are similar to those for the $(\alpha, 6n)$ reaction. Thus the spin populations do not depend much on whether neutrons are emitted at forward angles or backward angles and whether the neutron energies are high or low. They are all broad and about the same. It is clearly different from the results of HI reaction data. It indicates that the (α, xn) reaction may occur at the whole body of the nucleus. This interesting point will be discussed in the following section.

C. Angular momentum removed by the pre-equilibrium neutrons and angular momentum balance

Angular momentum transfers through the $(\alpha, xn\ \gamma)$ reactions are evaluated by following the same procedures as used in Ref. 9 and in the analysis of ^{164}Dy$(\alpha, xn\ \gamma)$ reactions with $E(\alpha) = 90$ MeV.[10,34]

Angular momenta carried away by the pre-equilibrium neutrons are evaluated as $l_n^p \approx \frac{1}{4} R P_n A_1^p n_p$, where P_n, n_p, and A_1^p are the mean momentum, mean multiplicity, and the coefficient of the $P_1(\cos\theta)$ term for the angular distribution of the pre-equilibrium neutrons, respectively, and R is the nuclear radius.[9] Since only the n_p neutrons out of the x neutrons contribute to the $A_1 P_1(\cos\theta)$ term, the value $A_1^p n_p$ may be obtained from the observed A_1(pe) value by using a relation A_1(pe) $= n_p A_1^p / x$. P_n was estimated from the observed average energy of the neutron emitted at the pre-equilibrium stage. R is obtained from $R = r_0(A_1^{1/3} + A_2^{1/3})$ with $r_0 = 1.2$ fm. Inserting the observed A_1(pe)$\cdot x$ and $\bar{E}_n$ values, one gets the values l_n^p as listed in the second columen of Table II. They are about one quarter of the average angular momentum (last column) introduced by the projectile. This does show quantitatively an important role of the pre-equilibrium neutrons for the angular momentum change as suggested by the fact that γ-ray multiplicity does not increase with increasing projectile energy far beyond the reaction threshold.[10-13] l_n^p values increase with decreasing the neutron multiplicity.

Angular momenta l_n^e carried away by the equilibrium (evaporating) neutrons were estimated by using a spin dependent level density

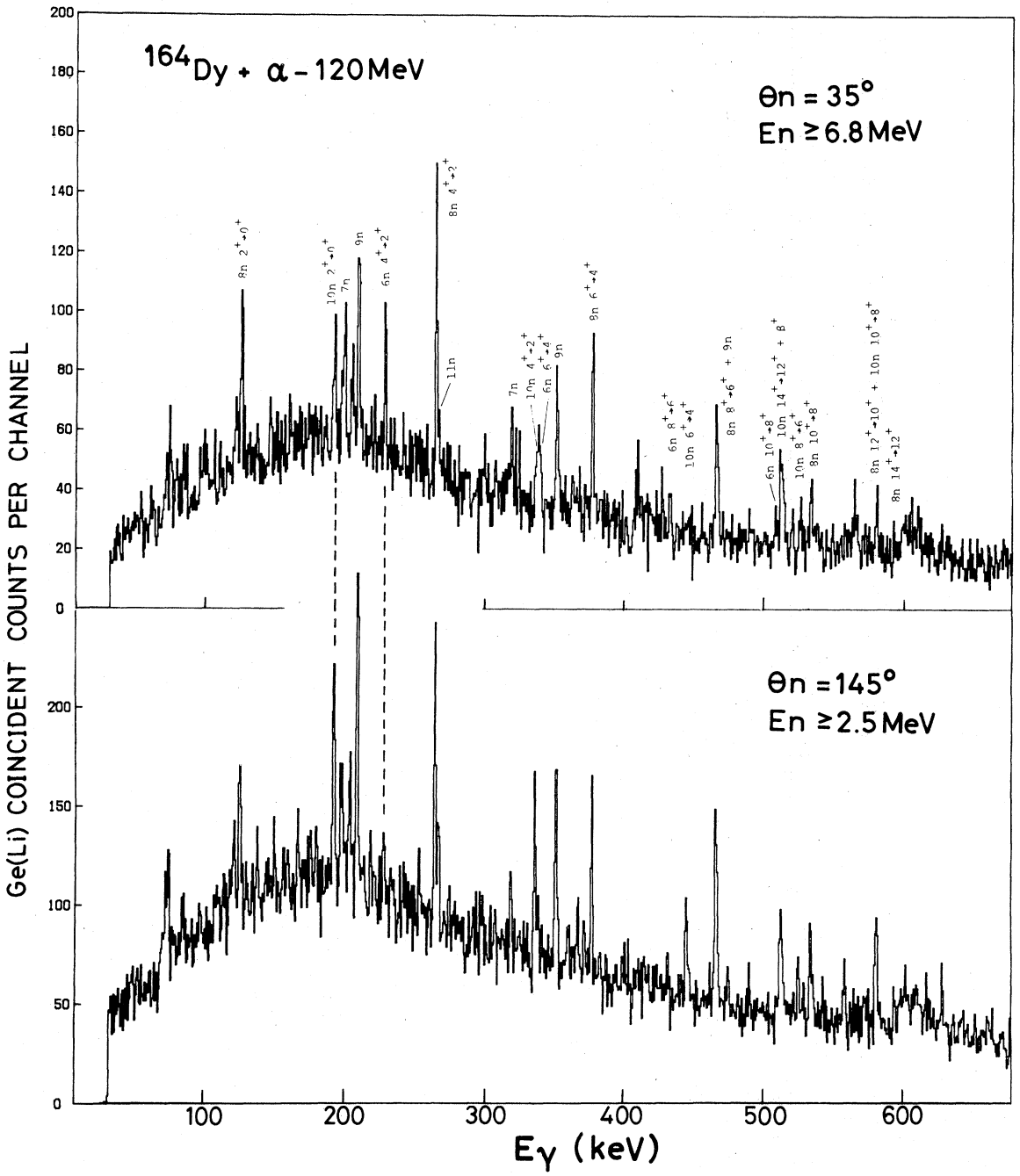

FIG. 8. γ-ray spectra gated by the fast neutron ($E_n \geq 6.8$ MeV) signals from the liquid scintillator at forward angle (35°) (upper spectrum) and gated by all neutron ($E_n \geq 2.5$ MeV) signals from the liquid scintillator at backward angle (145°) (lower spectrum). The $(\alpha, 6n)$ $4^+ \rightarrow 2^+$ transition and $(\alpha, 10n)$ $2^+ \rightarrow 2^+$ transition are noted by dashed lines to make clear the difference.

$$\rho(U, I) = \rho(U)(2I+1)\exp[-I(I+1)/2\sigma^2]$$

and the mean energy of the equilibrium neutrons. Here the spin cutoff parameters σ for the each reaction channel were evaluated by a relation $\sigma^2 = lT/\hbar^2$, where l is the rigid-body moment of inertia and T is the nuclear temperature.[31]

Angular momenta I_γ carried away by the γ rays were obtained from the γ-ray multiplicity data.[10] Thus the total angular momenta carried away

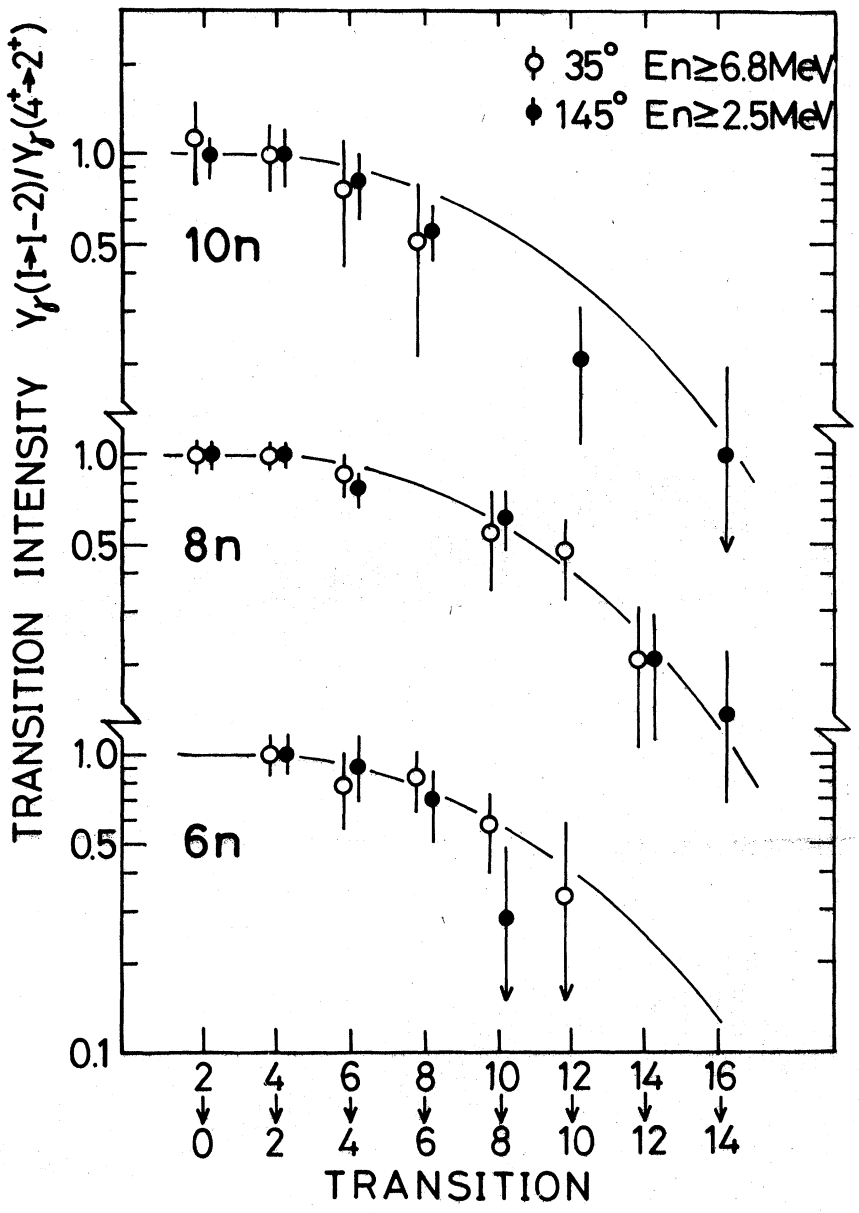

FIG. 9. γ-ray transition intensities relative to the $4^+ \to 2^+$ transition following the ^{164}Dy$(\alpha, xn)^{168-n}$Er reactions at $E(\alpha) = 120$ MeV. The upper, middle, and lower drawings are the data for the $(\alpha, 10n)$, $(\alpha, 8n)$, and $(\alpha, 6n)$ reactions, respectively. The open and full circles indicate the results gated by the high-energy neutrons alone ($E_n \geq 6.8$ MeV) in the liquid scintillator at the forward angle (35°) and the total neutrons ($E_n \geq 2.5$ MeV) at the backward angle (145°). The smoothed curves are drawn to show the relative transition intensities for the $(\alpha, 8n)$ reaction (see text).

through the $(\alpha, xn\ \gamma)$ reaction are given by

$$I = l_n^p + l_n^e + I_\gamma . \tag{2}$$

The estimated values are listed in Table II. Average angular momenta $\bar{I}$ introduced by the 120 MeV α projectile (last column) were obtained from $\bar{I} \approx \int P(I) I\, dI$, where the penetration coefficient $P(I)$ for the α projectile were estimated by using an optical potential. The value I carried away by the decaying neutrons and γ rays are nearly same for all reactions with $x = 6$–10, and are close to the value $\bar{I}$. Therefore all the $(\alpha, xn\ \gamma)$ reactions with $6n$ to $10n$ have almost same impact parameters around the mean nuclear radius $\frac{2}{3}R$.

It should be remarked that most previous works[11-13] on the angular momentum balance following the (particle, $xn\ \gamma$) reaction were discussed on the basis of the γ-ray multiplicity mea-

TABLE II. Angular momentum balance in $(\alpha, xn\,\gamma)$ reactions. l_n^p, l_n^e, and I_γ are angular momenta carried away by the neutrons emitted at the pre-equilibrium stage, neutrons emitted at the equilibrium stage, and deexciting γ rays. The I is the sum $l_n^p + l_n^e + I_\gamma$. All are given in units $\hbar$. The $\bar{I}$ is the average angular momenta introduced by the 120 MeV α projectile (see text).

Reaction	l_n^p	l_n^e	I_γ [a]	I	$\bar{I}$
$(\alpha, 10n)$	4.6 ± 1.2	3.2 ± 0.3	16 ± 1.5	23.8 ± 1.9	24.0
$(\alpha, 8n)$	5.8 ± 0.9	2.2 ± 0.3	15 ± 1.5	23.0 ± 1.8	24.0
$(\alpha, 6n)$	7.6 ± 2.3	1.6 ± 0.3	13 ± 1.5	22.2 ± 3.0	24.0

[a] From the results in Ref. 10.

surements alone. Angular momentum transfers in ^{165}Ho$(p, xn\,\gamma)$ reactions at $E_p = 60$ MeV have been obtained as $I = 11.6 \pm 1.5$ and $I = 9.8 \pm 1.5$ for the $(p, 4n)$ and $(p, 6n)$ reactions, respectively, which are close to the average input angular momentum estimated from the reaction cross section. A similar conclusion was also drawn for ^{164}Dy$(\alpha, xn\,\gamma)$ reactions at $E(\alpha) = 90$ MeV.[34]

IV. THE TWO PHASE DEEXCITATION MODEL AND NUMBER OF PRE-EQUILIBRIUM NEUTRONS

The present results may be analyzed as in Ref. 9 in terms of a simple two phase deexcitation process; one is the pre-equilibrium phase and the other the equilibrium phase. The n_p neutrons are assumed to be emitted isotropically with the Maxwell-Boltzmann distribution $E_n \exp(-E_n/T_p)$ in the center-of-mass system of the A' active exciton particles (local mass in an exciton number space) at the pre-equilibrium phase. T_p is the effective energy parameter. [Although the system is not equilibrated, one may call T_p the pre-equilibrium (quasi) temperature, for convenience.] The A' nucleons, corresponding to the local mass (hot active exciton particles at the pre-equilibrium stage), carry the linear momentum introduced by the α projectile. The energies and angles of the emitted neutrons in the center-of-local mass (A') frame were transformed into the energies and angles of the laboratory frame. Since the velocity of the local mass is rather large compared to the center-of-total mass (A) frame $(A' \ll A)$, the energies and angles of the emitted neutrons at the pre-equilibrium phase were on the average shifted to higher energies and to forward angles in the laboratory frame. This is really responsible for the forward peaking angular distribution in the laboratory system. These three parameters (n_p, T_p, A') were first derived from the calculations based on the exciton model.[32,33,36] The $x - n_p$ neutrons evaporated later on at the equilibrium phase were assumed to have a spectrum $E_n \exp(-E_n/T_e)$ in the center-of-total mass frame, where T_e is the nuclear temperature at the equilibrium phase. The neutron deexcitation processes throughout the (α, xn) reaction were simulated by a Monte Carlo method. This method was essential for feasible calculation of the complicated transformations from the center-of-local mass frame to laboratory frame through the neutron emissions. Overall fits to the observed data were obtained for a set of parameters $n_p = 1.7$, $A' = 12$, $T_p = 6$ MeV and $T_e = 1.6$ MeV (see Figs. 2 and 4). These values were consistent with the exciton model estimation.[32,33] Here the calculated total (α, xn) reaction cross section σ_n was normalized so as to give $\sigma_n = \sum_n \sigma(\alpha, xn)$, where $\sigma(\alpha, xn)$ is the observed (α, xn) cross section (Fig. 2). The energy spectra and an angular distributions were significantly affected by the change of these parameters.

It should be noted that this simple model with only three parameters for the pre-equilibrium process reproduces not only the cross sections of the individual reaction channel but also the energy spectra and angular distributions of neutrons in every reaction channel. Although this fact does not provide a definitive test of this simple two phase deexcitation model, it describes the deexcitation process very nicely.

Finally some remarks should be made on the comparison with other phenomenological models, a nuclear fireball model[37] and a hot spot model.[38] The nuclear fireball model[37] was proposed to help us understand the spectra for products from relativistic heavy-ion collisions of hundreds of MeV/nucleon. The nucleons which are mutually swept out from both the target nucleus and the projectile form a hot quasiequilibrated fireball and decay as an ideal gas. The model reproduces well the overall features of the inclusive spectra from relativistic heavy-ion collisions. Our simple two phase deexcitation model is essentially similar to the idea of the fireball model except for the following two points: First, the impact parameter is important in the fireball model, while our model has no such parameter. Second, the $\sqrt{E}$ is used as the pre-exponential factor in the Maxwell-Boltzmann distribution, while we have used a conventional factor E.[39] The former corresponds to a volume Maxwellian $[\sqrt{E} \cdot \exp(-E/T)]$ and the latter to a evaporating Maxwellian $[E \cdot \exp(-E/T)]$.

Another phenomenological model[38] called a hot spot has been formulated in a completely different way to analyze the pre-equilibrium behavior in deep inelastic collisions of heavy ions of about 10 MeV/nucleon. The excitation energy created by the projectile at the nuclear surface is localized in both space and time, and it subsequently decays via

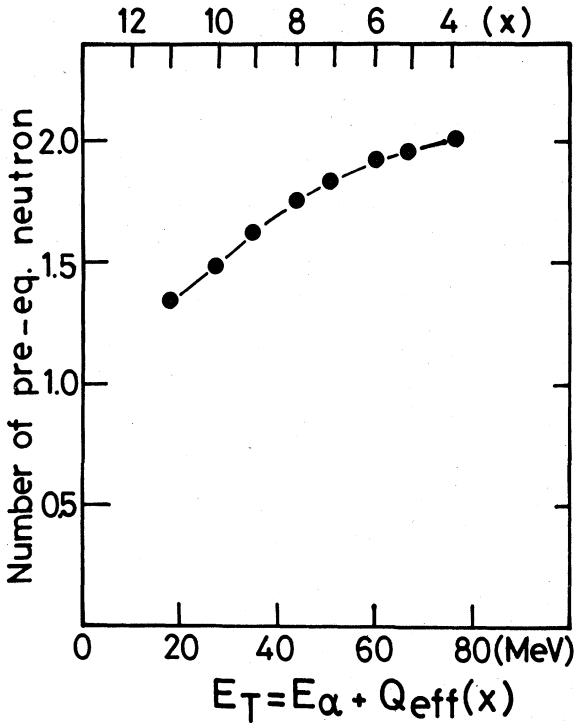

FIG. 10. Number of the pre-equilibrium neutrons as a function of the energy sum E_T of the emitted neutrons and/or the neutron multiplicity. These values are calculated on the basis of a simple two phase deexcitation model (see text).

diffusion of heat in the nuclear matter. In this model, rather elaborate calculations would be needed to obtain the numerical results. The predicted temperatures for neutron energy spectra from the reaction of 96 MeV ^{16}O on ^{58}Ni were 8–9 MeV (Ref. 40) and they are slightly higher than ours, ~6 MeV. The difference may be due to the mass difference. It is interesting to apply more sophisticated analysis such as the multistep direct-reaction (MSDR) method developed by Tamura *et al.*[41]

The number n_p of the pre-equilibrium neutrons for the individual reaction channel is calculated by using the simple two phase deexcitation model. The number n_p is plotted as a function of the neutron multiplicity x and/or the total kinetic energy E_T in Fig. 10. Even in the $(\alpha, 10n)$ reaction 1.5 neutrons are emitted at the pre-equilibrium phase and the n_p increases as the neutron multiplicity decreases from 10 to 4. In the $(\alpha, 6n)$ channel almost 2 neutrons are emitted at the pre-equilibrium phase.

The number n_p of the pre-equilibrium neutrons for the ^{165}Ho$(p, xn\ \gamma)$ reactions at $E_p = 60$ MeV varies drastically from 0.6 for the $(p, 6n)$ reaction to 1.9 for the $(p, 2n)$ reaction.[9] The difference is considered to be due to the different number of excitons at the initial stage and the large projectile energy per nucleon. The number of the pre-equilibrium nucleons or α particle is also obtained by several investigators.[1,13,42,43] For the high-energy projectile the n_p value was obtained by Sadler *et al.*[42] from the systematics of variation of production cross section by observing singles γ-rays spectra following bombardment of several medium mass nuclei with intermediate-energy protons $[E(p) = 80–160$ MeV]. They conclude that one or two nucleons are emitted in the pre-equilibrium phase. Sarantites *et al.*[13] obtained the n_p value by comparing their γ-ray multiplicity data following the ^{166}Er$(\alpha, xn\ \gamma)$ reactions $E(\alpha) = 95.3$ MeV with the geometry-dependent hybrid model calculations. They obtained more than one pre-equilibrium neutron emission event. By observing the energy and angular distributions of the decaying particles, the n_p values have also been obtained. Assuming that the neutron yield at backward angles is mostly due to the compound process, and the high-energy parts of the neutron spectra at the forward angles are mostly due to the pre-equilibrium process (in Sec. III), the n_p values were deduced phenomenologically from the forward-backward difference of differential cross sections as shown in Refs. 16 and 42. The results of Westerberg *et al.*[16] indicate a substantial decrease of the n_p in going from the $8n$ to the $10n$ channel following the ^{158}Gd + ^{12}C MeV reactions at $E(^{12}C) = 152$ MeV. They also obtained the n_p values for the ^{158}Gd$(^{12}$C$, \alpha xn\ \gamma)$ reaction channels. It is worthwhile to point out that one should be careful to deduce the number of the pre-equilibrium particles n_p from the forward-backward differences, since the energy spectrum even at backward angles contains the significant contributions from the pre-equilibrium process as displayed in Fig. 4. Yet these results are generally consistent with our data.

V. SUMMARY AND CONCLUDING REMARKS

Cross sections and neutron energy and angular distributions for the ^{164}Dy$(\alpha, xn\ \gamma)$ reactions were carefully measured as a function of neutron multiplicity x in a wide range of $x = 4–12$, and characteristic behaviors of the pre-equilibrium process were clearly found. The following results were obtained from the detailed analysis of the γ-ray spectrum and from the n-γ coincidence work:

(i) The (α, xn) reaction cross section deviate much from the expectation for the equilibrium evaporation process, and a tail for the small x due to the deviation corresponds to the pre-equilibrium process.

(ii) A high-energy (10–15 MeV) component and a

low-energy (~2 MeV) evaporation pattern were found in the neutron energy spectra. The former is enhanced at forward angles and in the reaction with the small x of emitted neutrons.

(iii) All (α, xn) reaction channels ($x = 6-11$) have pre-equilibrium neutrons with forward peaking angular distributions. The asymmetric coefficient A_1 for the individual reaction channel increases gradually with the decreasing number x of emitted

These pronounced effects due to the pre-equilibrium process are obtained by using the higher bombarding energy 30 MeV/nucleon and selecting reaction channels with large $\bar{E}_n$ values (small neutron multiplicity x). Note that for the $(\alpha, 6n)$ reaction $\bar{E}_n \approx 10$ MeV. These features are naturally different from the other neutron experiments following (HI, xn) reactions as follows: For the ^{158}Gd(^{12}C, xn γ) reaction[16] at $E(^{12}\text{C}) = 152$ MeV the bombarding energy is 12.7 MeV/nucleon, and the $\bar{E}_n$ values for the (^{12}C, $8n$) and (^{12}C, $10n$) reaction channel are 6 and 3.1 MeV, respectively. It is interesting to note that even at this low bombarding energy the pre-equilibrium process was found in the neutron spectra.

We have demonstrated that the asymmetry coefficient A_1 gives an angular momentum removed by the pre-equilibrium neutrons. Combined with the data of the γ-ray multiplicity we obtained important information on the angular momentum balance in the $(\alpha, xn\ \gamma)$ reactions. The angular momentum transfers for the $6n$ to $10n$ reactions obtained by using the A_1 and the γ-ray multiplicity show almost the same values and are close to the mean angular momentum introduced by the 120 MeV α particles. It may indicate that the (α, xn) reactions proceed through the whole nucleus. In other words, the mean impact parameter is approximately given by the mean radius $\frac{2}{3}R$.

Simple calculations were carried out in terms of the two phase deexcitation model, the pre-equilibrium process followed by the equilibrium process. Neutron energy spectra as well as angular distributions were reproduced as a function of neutron multiplicity. Here we have assumed for the pre-equilibrium process n_p neutrons emitted isotropically in the center of mass of the local exciton particles (local mass A') with a energy spectrum of a Maxwell-Boltzmann distribution $E_n \cdot \exp(-E_n/T_p)$, where T_p is the energy parameter (pre-equilibrium temperature). At the beginning these three parameters (n_p, T_p, A') were estimated by using the exciton model calculations. This pre-equilibrium phase is followed by neutron evaporation with a nuclear temperature T_e at the equilibrium phase. The following values were used for the present calculation: $n_p = 1.7$, $T_p = 6$ MeV, $A' = 12$, and $T_e = 1.6$ MeV. The number of the pre-equilibrium neutrons for the individual reaction channel was also obtained by using this simple model.

In short, the nucleus excited by the 120 MeV α projectile deexcites down to 90–60 MeV by emitting 1.5–2 fast neutrons with $T_p = 6$ MeV and the average exciton particle number 12 at the pre-equilibrium phase, and then cools down by evaporating 8–4 neutrons at the equilibrium phase. The angular momentum removed by the neutrons emitted at the pre-equilibrium phase was found to be roughly $l_n^p = 6-8\hbar$.

Finally it should be remarked that the cross sections for the $(\alpha, pxn\ \gamma)$ and $(\alpha, \alpha' xn\ \gamma)$ reactions[44] at present energy amount to 35% and 15% of the total reaction cross section, respectively. It is interesting to study the charged particle energy spectra and angular distributions in coincidence with residual γ rays, since charged particles are considered to be emitted mainly at the pre-equilibrium stage, and it may be useful for clarifying the reaction mechanism. It is also interesting to extend systematically this work to higher projectile energies and to weakly bound projectiles (d, ^{3}He) or heavy ion, where the projectile break-up process[45] or high angular momentum introduced by the projectile play an important role.

ACKNOWLEDGMENTS

The authors are very grateful to Professor S. Yoshida for valuable discussions and to Professor S. Yamabe for criticism and encouragement. We also wish to thank the RCNP staffs and the cyclotron crew for their generous support during the experiment.

---

*Concurrent with the RCNP, Osaka Univ.

[1]M. Blann, Annu. Rev. Nucl. Sci. 25, 123 (1975), and references therein.
[2]H. W. Broek, Phys. Rev. 124, 233 (1961).
[3]W. G. Simon and S. T. Ahrens, Phys. Rev. C 2, 1292 (1970).
[4]Y. Eyal, A. Gavron, I. Tserruya, Z. Fraenkel, Y. Eisen, S. Wald, R. Bass, G. R. Gould, G. Kreyling, R. Renfordt, K. Stelzer, R. Zitzmann, A. Gobbi, U. Lynen, H. Stelzer, I. Rode, and R. Bock, Phys. Rev. Lett. 41, 625 (1978).
[5]S. M. Grimes, J. D. Anderson, J. C. Davis, and

C. Wong, Phys. Rev. C 8, 1770 (1973).
[6]A. Alevra, R. Dumitrescu, I. R. Lukas, M. T. Magda, D. Plostinaru, E. Trutia, N. Chevarier, A. Chavarier, A. Demeyer, and Tran Minh Duc, Nucl. Phys. A209, 557 (1973).
[7]A. Chevarier, N. Chevarir, A. Demeyer, A. Alevra, R. Dumitrescu, I. R. Lukas, M. T. Magda, and M. E. Nistor, Nucl. Phys. A231, 64 (1974).
[8]M. Blann, R. R. Doering, A. Galonsky, D. M. Patterson, and F. E. Serr, Nucl. Phys. A257, 15 (1976).
[9]H. Ejiri, T. Shibata, T. Itahashi, T. Nagai, H. Sakai, S. Nakayama, T. Kishimoto, K. Maeda, and M. Hoshi, Nucl. Phys. A305, 167 (1978); J. Phys. Soc. Japan Suppl. 44, 655 (1978).
[10]Y. Nagai, T. Shibata, H. Sakai, T. Kishimoto, and H. Ejiri, J. Phys. Soc. Japan 46, 1025 (1979).
[11]M. Ogawa, P. Kleinheinz, S. Lunakdi, O. W. Schult, and M. Fenzl, Z. Phys. A284, 271 (1978).
[12]W. J. Ockels, M. J. A. de Voigt, and Z. Sujkowski, Phys. Lett. 78B, 401 (1978); M. J. A. de Voigt, private communication (1978).
[13]D. G. Sarantites, L. Westerberg, R. A. Dayras, M. L. Halbert, D. C. Hensley, and J. H. Barker, Phys. Rev. C 17, 601 (1978); 18, 774 (1978).
[14]H. Suzjki *et al.*, private communication.
[15]H. Ejiri *et al.*, private communication.
[16]L. Westerberg, D. G. Sarantites, D. C. Hensley, R. A. Dayras, M. L. Halbert, and J. H. Barker, Phys. Rev. C 18, 796 (1978).
[17]S. A. Hjorth, H. Ryde, K. A. Hagemann, G. Lovhoiden, and J. C. Waddington, Nucl. Phys. A144, 513 (1970).
[18]E. Grosse, F. S. Stephens, and R. M. Diamond, Phys. Rev. Lett. 31, 840 (1973).
[19]R. M. Lieder, H. Beuscher, W. F. Davidson, P. Jahn, H. J. Probst, and C. Mayer-Böricke, Z. Phys. 257, 147 (1972).
[20]R. Janssens, Y. El Masri, J. M. Ferte, C. Michel, J. Steyaert, and J. Vervier, Nucl. Phys. A283, 493 (1977).
[21]O. C. Kistner, A. W. Sunyar, and E. der Mateosian, Phys. Rev. C 17, 1417 (1978).
[22]J. K. Tuli, Nucl. Data Sheets 9, 435 (1973); 12, 477 (1974); 13, 493 (1974).
[23]A. Buyrn, Nucl. Data Sheets 11, 327 (1974); 17, 97 (1976).
[24]R. Broda, M. Ishihara, B. Herskind, H. Oeschler, S. Ogaza, and H. Ryde, Nucl. Phys. A248, 356 (1976).
[25]P. Sperr, H. Speler, M. R. Maier, and D. Evers, Nucl. Instrum. Methods 116, 55 (1974).
[26]V. V. Verbinski, W. R. Burrus, T. A. Love, W. Zobel, N. W. Hill, and R. Textor, Nucl. Instrum. Methods 65, 8 (1968).
[27]H. W. Broek and C. E. Anderson, Rev. Sci. Instrum. 31, 1063 (1960).
[28]I. Katayama and H. Ogata, RCNP Annual Report, 1976 (unpublished), p. 153.
[29]H. Sakai, K. Maeda, and H. Ejiri, Nucl. Instrum. Methods (to be published).
[30]A. Bohr and B. Mottelson, *Nuclear Structure* (Benjamin, New York, 1969), Vol. 1.
[31]T. E. Ericson, Adv. Phys. 9, 425 (1960).
[32]H. Sakai, H. Ejiri, T. Kishimoto, and S. Yoshida, in Proceedings of the International Symposium on Heavy-ion and Pre-equilibrium Reactions, The Institute of Physical and Chemical Research, Wako-Shi-Saitama, Japan, 1977 (unpublished), Suppl. 6, p. 400.
[33]H. Sakai, H. Ejiri, and S. Yoshida, Phys. Rev. C (to be published).
[34]H. Ejiri *et al.*, Nucl. Phys. (to be published).
[35]T. Inamura, M. Ishihara, T. Fukuda, T. Shimoda, and H. Hiruta, Phys. Lett. 68B, 51 (1977).
[36]S. Yoshida, in Proceedings of the International Symposium on Heavy-Ion and Pre-equilbrium Reactions, IPCR 1977 (unpublished), Suppl. 6, p. 359.
[37]G. D. Westfall, J. Gosset, P. J. Johansen, A. M. Poskanzer, W. G. Meyer, H. H. Gutbrod, A. Sandoval, and R. Stock, Phys. Rev. Lett. 37, 1202 (1976).
[38]R. Weiner and M. Weström, Phys. Rev. Lett. 34, 1523 (1975).
[39]A. S. Goldhaber, Phys. Rev. C 17, 2243 (1978).
[40]P.-A. Gottschalk and M. Weström, Phys. Rev. Lett. 39, 1250 (1977).
[41]T. Tamura, T. Udagawa, D. H. Feng, and K.-K. Kan, Phys. Lett. 66B, 109 (1977).
[42]M. Sadler, J. Jastrzebski, A. Nadasen, P. O. Singh, L. L. Rutledge Jr., T. Chen, and R. E. Segel, Phys. Rev. Lett. 38, 950 (1977).
[43]C. R. Lux and N. T. Porile, Phys. Rev. C 18, 138 (1978).
[44]K. Okada *et al.* and T. Shibata *et al.* to be published.
[45]A. Shimizu *et al.*, to be published.